Journal of Alloys and Compounds 929 (2022) 167279

Contents lists available at ScienceDirect

Journal of Alloys and Compounds

journal homepage: www.elsevier.com/locate/jalcom

Ferromagnetism in Pr-rich binary Pr_7Ru_3 intermetallic compound

S. Królak [a,b], H. Świątek [a,b], K. Górnicka [a,b], M.J. Winiarski [a,b], W. Xie [c], R.J. Cava [d], T. Klimczuk [a,b,*]

[a] Faculty of Applied Physics and Mathematics, Gdansk University of Technology, Narutowicza 11/12, 80-233 Gdansk, Poland
[b] Advanced Materials Centre, Gdansk University of Technology, Narutowicza 11/12, 80-233 Gdansk, Poland
[c] Department of Chemistry and Chemical Biology, Rutgers University, Piscataway, NJ 08854, USA
[d] Department of Chemistry Princeton University, Princeton, NJ 08540, USA

ARTICLE INFO

Article history:
Received 20 July 2022
Received in revised form 5 September 2022
Accepted 19 September 2022
Available online 21 September 2022

Keywords:
Synthesis
Ferromagnetism

ABSTRACT

We present the synthesis and experimental characterization of the binary intermetallic compound Pr_7Ru_3. The polycrystalline sample was prepared by arc melting pure Pr and Ru, followed by homogenization at 500 °C and 600 °C for 48 and 89 h, respectively. Powder x-ray diffraction confirms that Pr_7Ru_3 crystallizes in an orthorhombic crystal structure (Pnma, space group no. 62) with the lattice parameters: a = 7.3606(7) Å, b = 23.120(1) Å and c = 6.5959(5) Å. Magnetization, resistivity, and heat capacity measurements reveal a ferromagnetic transition in Pr_7Ru_3 with the Curie temperature $T_C \sim 24.5$ K. The bulk transition is confirmed by a large λ-shape anomaly observed in the specific heat measurement. The magnetic susceptibility above the transition obeys the modified Curie-Weiss law with a positive Curie-Weiss temperature $\Theta_{CW} = 30(1)$ K and an effective magnetic moment of 3.39(1) μ_B/Pr. Resistivity data for Pr_7Ru_3 reveals metallic-like behavior with a clear anomaly at the transition temperature which is smeared by an applied magnetic field. We also synthesized high-quality nonmagnetic analog La_7Ru_3 for which superconducting transition is observed with $T_c = 1.95$ K, in agreement with the literature.

1. Introduction

Intermetallic binary compounds based on a combination of rare-earth (RE) and transition metals (T) from groups 8, 9, and 10 exhibit many interesting physical phenomena, including different types of magnetic ordering [1–7] and superconductivity [8–15]. One of the most well-known structures for such binaries are Laves phases which are important in engineering applications, such as a hydrogen storage system [16]. However, one family of compounds has not drawn too much attention from the materials community – the Th_7Fe_3 type. From the chemistry perspective, the rare-earth elements have larger electropositivity than the late transition metals, which results in filling the *d* orbitals on the late transition metals when they form intermetallic compounds. Similar electronic interactions were observed in $FeGa_3$ – a small gap Kondo-like system [17,18]. Thus, it motivates us to study the binary phases forming between rare-earth and transition metals and to examine the *f* - *d* interactions in the materials.

Rare-earth-based binary ruthenides form in the chemical stoichiometry that ranges from ruthenium-rich $RERu_2$ to rare-earth-rich RE_3Ru. RE_7Ru_3 compounds with the Sr_7Pt_3 type crystal structure are reported only for La, Pr, and Nd, while for Ce the structure is of the Th_7Fe_3 type [19]. The crystal structure of Pr_7Ru_3 is relatively complex, featuring 4 inequivalent Pr positions, each having different coordination and connectivity and hence different local site symmetry. As a result, a complicated crystal field splitting of Pr^{+3} is expected. The sublattice of Pr atoms forms a 3-dimensional network with the nearest-neighbor Pr-Pr distance varying from 3.6 Å to 4 Å. In the RE_7Ru_3 family, the physical properties depend on the type of RE ion: La_7Ru_3 is reported to be a superconductor with $T_c = 1.93$ K [20], Ce_7Ru_3 is an antiferromagnet exhibiting non-Fermi liquid behavior [21], while for Nd_7Ru_3 and Pr_7Ru_3 physical properties have not been described.

The interplay between exchange interaction and crystalline field in compounds containing light rare-earth atoms is, to this day, not well understood, as not all of the reported compounds are fully characterized. In this project, we report the magnetic, thermal and electronic transport properties of Pr_7Ru_3 for the first time, with an aim to broaden the understanding of magnetic interactions in rare-earth transition metal intermetallic systems. We find a ferromagnetic transition in Pr_7Ru_3 with the Curie temperature $T_C = 24.5$ K, as

* Corresponding author at: Faculty of Applied Physics and Mathematics, Gdansk University of Technology, Narutowicza 11/12, 80-952 Gdansk, Poland.
E-mail addresses: hanna.swiatek@pg.edu.pl (H. Świątek), tomasz.klimczuk@pg.edu.pl (T. Klimczuk).

https://doi.org/10.1016/j.jallcom.2022.167279

determined by specific heat measurement. Since ferromagnetism in rare-earth-based metallic systems is less common than the occurrence of antiferromagnetism [22], Pr_7Ru_3 appears to be especially interesting.

2. Experimental

The Pr_7Ru_3 sample was prepared by melting stoichiometric amounts of pure Pr (Alfa Aesar, 99.9 %) and Ru (Alfa Aesar, 99.95 %) pieces under an argon atmosphere in an arc-melting furnace (MAM-1 Edmund Buhler GmbH), with zirconium used as a getter. The sample button was melted four times to improve the reaction between the constituents. There was no significant weight loss after the process. The sample was then wrapped in Ta foil, sealed in an evacuated quartz tube, and annealed at 500 °C for 48 h and then 600 °C for 89 h.

Phase purity and structural data for the sample were checked by powder x-ray diffraction at room temperature, using a Bruker D2 Phaser 2nd generation diffractometer with CuK_α radiation (λ = 1.5404 Å) and XE-T detectors. The unit cell parameters were refined in Bruker Topas software employing the LeBail method.

All the measurements were performed using an Evercool II Quantum Design Physical Property Measurement System (PPMS). Resistivity was determined using a four-terminal technique, with 50 µm-diameter platinum wire leads spark-welded to the sample surface. The specific heat was measured in the applied field ranging from 0 to 1 T, using the two-τ relaxation method. For magnetic measurements, the vibrating sample magnetometer (VSM) function was employed. Field-dependent magnetization at 2 K and temperature-dependent magnetic susceptibility were measured, including dependencies of zero-field cooled and field cooled magnetizations in various fields. Throughout the text, the magnetic susceptibility was approximated as $\chi \approx M/H$.

3. Results and discussion

The Pr_7Ru_3 sample was first characterized by room temperature powder X-ray diffraction (pXRD). The pXRD pattern together with

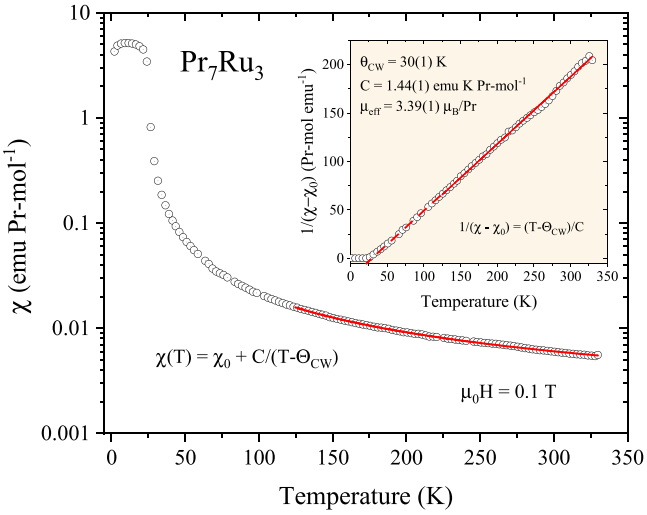

Fig. 2. Temperature dependence of magnetic susceptibility of Pr_7Ru_3 sample. Points represent experimental data and the solid red line is a modified Curie-Weiss fit. In the inset, the inverse susceptibility versus temperature is shown, with a linear fit (solid red line) used to determine the Curie constant and temperature, as well as the effective magnetic moment. The dashed line is a guide to the eye.

LeBail refinement is shown in Fig. 1, represented by open circles and solid red line, respectively. The Bragg positions (vertical bars) and the difference plot between experimental and fitted data (blue line) are also shown. The compound was found to be a single phase with no extra peaks that might correspond to possible impurities. All reflections are indexed in the orthorhombic Sr_7Pt_3-type structure (Pnma, s.g. no. 62) with lattice parameters a = 7.3606(7) Å, b = 23.120(1) Å and c = 6.5959(5) Å. These values are in very good agreement with the crystallographic data published previously [19]. The detailed discussion of the Sr_7Pt_3-type structure can be found in [23].

The temperature-dependent and field-dependent magnetization and magnetic susceptibility of Pr_7Ru_3 were analyzed in detail. Fig. 2 presents the temperature dependence of magnetic susceptibility

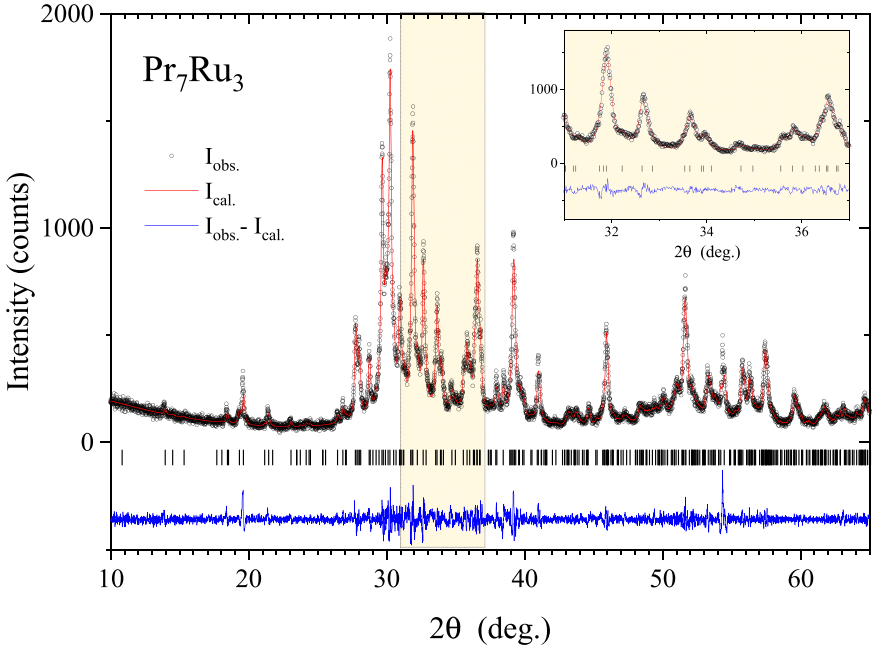

Fig. 1. Powder x-ray diffraction pattern of Pr_7Ru_3. Points represent experimental data and solid red line is the LeBail fit. Difference line is shown below (blue), as well as expected peak positions corresponding to hkl planes (black vertical bars). The LeBail refinement confirms the previously reported values of lattice constants as well as the sample space group.

χ(T), measured in an applied field of 0.1 T. The vertical axis is presented on a logarithmic scale. There is a significant rise in susceptibility in the low-temperature region, which is a hint of possible ferromagnetism [24–30]. The inverse susceptibility, $1/(\chi - \chi_0)$, temperature dependence is shown in the inset of Fig. 2. The χ(T) experimental data points were fitted with a modified Curie-Weiss (CW) law, by using the formula: $\chi(T) = \chi_0 + C/(T - \Theta_{CW})$ in the temperature range 125 – 325 K. A fit shown in the main panel of Fig. 2 by a red solid line yielded the independent susceptibility term $\chi_0 = 7.2(4) \times 10^{-4}$ mol-Pr^{-1}, Curie constant C = 1.44(1) emu K Pr-mol^{-1} and Curie-Weiss temperature $\Theta_{CW} = 30(1)$ K. A positive value of Θ_{CW} indicates the presence of the ferromagnetic interactions at high temperatures. With the obtained Curie constant and with the assumption, that the magnetic moment comes solely from trivalent praseodymium ions Pr^{3+}, the effective magnetic moment per Pr was calculated from the expression: $\mu_{eff} = \sqrt{\frac{3Ck_B}{\mu_B^2 N_A}}$, where k_B is the Boltzmann constant, μ_B is the Bohr magneton and N_A is Avogadro's constant. The estimated effective magnetic moment is $\mu_{eff.} = 3.39(1)$ μ_B/Pr, which is close to the expected value for Pr^{3+} ion of 3.58 μ_B [24] and suggests that the sole origin of magnetism is the rare-earth metal.

In order to analyze how the applied magnetic field interacts with the sample, we measured zero-field cooled (ZFC) and field cooled (FC) magnetic susceptibility in applied fields of 1 mT, 10 mT, 100 mT, and 1 T, as shown in Fig. 3. In each case, below 30 K, a significant rise of the χ(T) is observed, which is a sign of ferromagnetic behavior. The transition is sharp for the lowest applied field and smears as the field

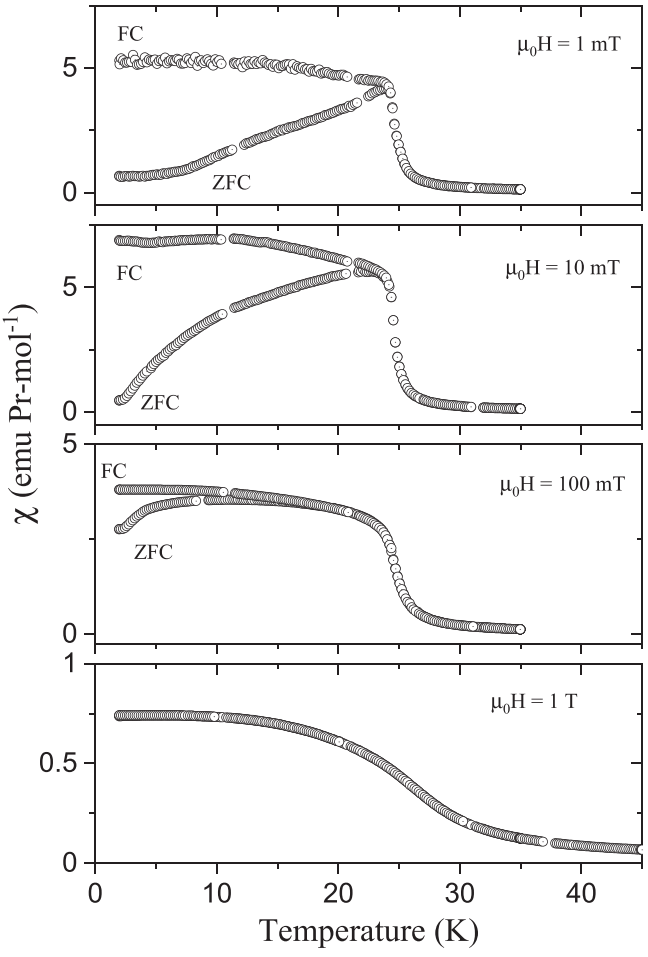

Fig. 3. Zero field cooled and field cooled susceptibility curves versus temperature, shown between 0 and 45 K for fields of 1, 10, 100 mT and 1 T.

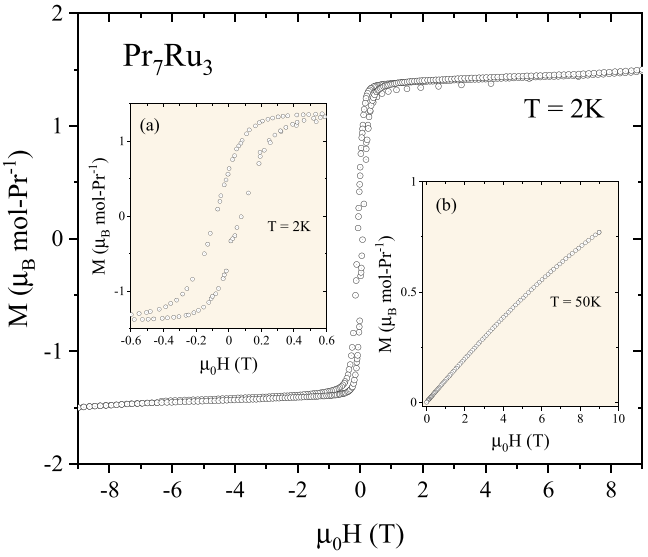

Fig. 4. Field-dependent magnetization of the sample, measured in isothermal conditions and the field range of –9 T to 9 T. The left inset shows a more detailed look at the hysteresis loop, while the right shows the magnetic moment above Curie temperature with visible paramagnetic behavior.

increases. A rough estimation of the transition from the minimum of dχ/dT, for the lowest used field $\mu_0 H = 1$ mT, gives $T_C = 24.6$ K. For the fields lower than 1 T, the ZFC and FC curves are visibly separated, which is likely a result of domain wall pinning, due to the presence of magnetocrystalline anisotropy, which is a common feature in the rare-earth compounds [24,31,32]. The observed overlap of ZFC and FC curves at 1 T is due to the fact that the magnetization is essentially fully saturated at this field, i.e., all moments/domains are aligned.

An important measurement in the case of a compound that is tested for possible ferromagnetism or spin glass behavior is the field-dependent magnetization M(H) below the Curie temperature. The main panel and the left inset of Fig. 4 present M(H) data points for Pr_7Ru_3 collected at T = 2 K. The ferromagnetic character is clearly visible, with a closer look at the hysteresis loop shown in Fig. 4(a). The estimated coercivity field for Pr_7Ru_3 is $\mu_0 H_C = 0.08$ T and the remnant magnetization $\mu_R = 0.6$ μ_B/mol-Pr, which is roughly 40 % of the magnetization in the maximum applied field of 9 T. The magnetization curve M(H) tends to saturate, however, the powder-averaged $M_{2\,K} \sim 1.4$ μ_B is far lower than expected for a 9-fold degenerate manifold of Pr^{+3} (3.2 μ_B). The M(H) slope calculated between 2 T and 9 T is $M/H = 6.5(6) \times 10^{-3}$ emu mol-Pr^{-1}. A lower-than-expected value of saturated moment (2.57 μ_B) was also found in the Laves $PrAl_2$ [33]. This is likely caused by the single-ion anisotropy effects and we return to this point in a discussion of magnetic entropy. In the light rare-earth-based intermetallics, the crystalline electric field (CEF) may play a significant role [24,34,35], as well as the random distribution of easy and hard magnetization axes due to the sample's polycrystalline structure [36]. In the case of Pr_7Ru_3, with four inequivalent Pr sites, CEF effects are particularly complex. All of the above may cause a lower-than-expected saturation value. The M(H) measured at 50 K is presented in Fig. 4(b). As expected, above the Curie temperature, ferromagnetic behavior is no longer visible and M(H) becomes a straight line with only small curvature above 6 T, which is typical for paramagnetic compounds.

To further analyze the magnetic properties of Pr_7Ru_3, specific heat measurements were conducted. The main panel of Fig. 5(a) presents the temperature dependence of the specific heat C_p/T for Pr_7Ru_3 (red line) and La_7Ru_3 (blue line) in the whole temperature range. The data were collected in a zero applied field. The inset of Fig. 5(a) shows C_p/T vs. T in the low-temperature region surrounding

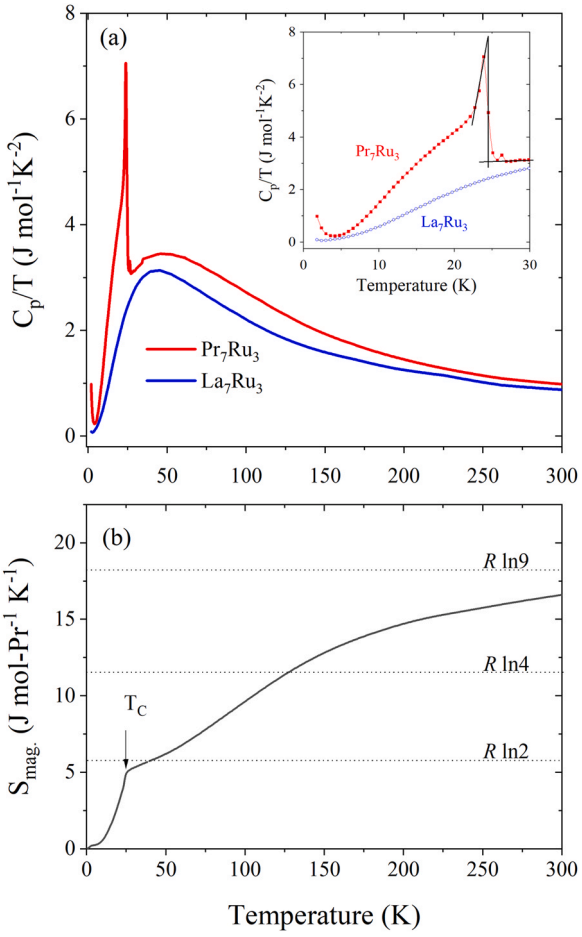

Fig. 5. (a) Temperature dependence of the specific heat C_p/T for both Pr_7Ru_3 and La_7Ru_3. Detailed studies of the specific heat in the vicinity of superconducting transition for La_7Ru_3 is provided in SI. (b) Magnetic entropy S_{mag} of Pr_7Ru_3. The vertical arrow indicates the Curie temperature T_C = 24.5 K.

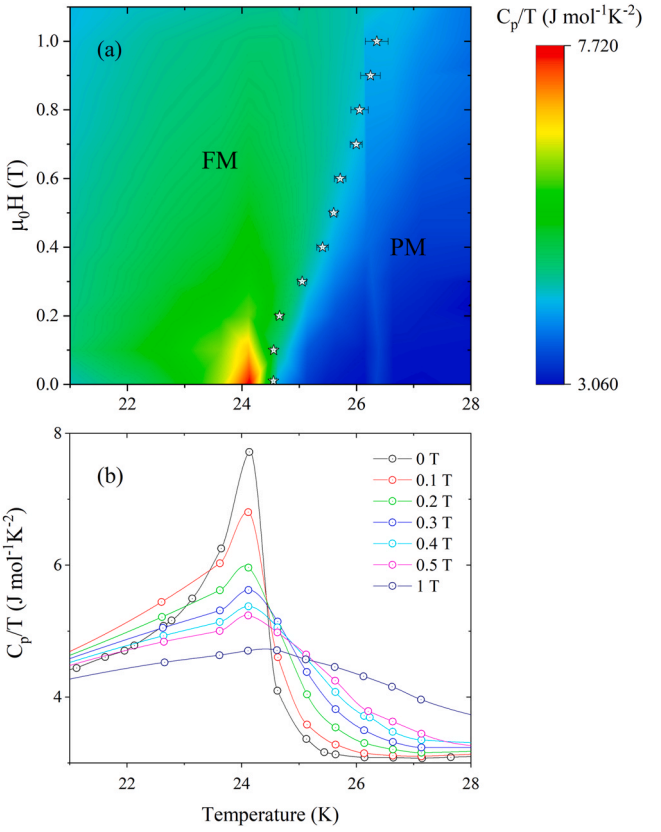

Fig. 6. (a) Specific heat map, showing its temperature dependence near transition temperature in the applied field range of 0–1 T. The white points indicate the minima of the first derivative of magnetic susceptibility with respect to the temperature, corresponding to the phase transition temperature. (b) Heat capacity (C_p/T) vs. temperature measured in zero field (open black circles) and under various magnetic fields.

the transition. Near 25 K a distinct lambda-shape anomaly for Pr_7Ru_3 is seen, which is associated with a second order phase transition and confirms bulk nature of the transition. A second order phase transition is also suggested by the lack of thermal hysteresis in the resistivity data (not shown). The low-temperature upturn seen below 3.5 K is likely a nuclear Schottky effect (C_N). This conclusion comes from the observation and detailed discussion of a high C_N anomaly at the same temperature range for $PrAl_2$ [37].

The magnetic contribution ($C_{mag.}$) to the specific heat can be estimated using a comparative analysis with a non-magnetic isostructural compound. Here, La_7Ru_3 was chosen as the analog material, as it forms in the same crystal structure, has similar lattice parameters to Pr_7Ru_3 and, what is equally important, the molar mass of La is only 1.4 % less than that of Pr. Detailed analysis of the C_p for a non-magnetic La_7Ru_3 compound in the vicinity of the superconducting transition is presented in the SI. The $C_{mag}(T)$ was obtained by subtracting the experimental $C_p(T)$ for La_7Ru_3. Next, the magnetic entropy $S_{mag}(T)$ was calculated from the obtained magnetic specific heat by numerical integration of C_{mag}/T, and the result is shown in Fig. 5(b). The contribution of the nuclear Schottky anomaly to the specific heat (seen below 3.5 K) was neglected which slightly overestimates S_{mag} [38,39]. There is a clear change of the $S_{mag}(T)$ behavior near T_C and the entropy released up to 24.5 K is S_{mag} = 5 J Pr-mol^{-1} K^{-1}. This value is much lower than *R*ln9 but reasonably matches with *R*ln2 and hence the suggested ground state for Pr_7Ru_3, due to the $4f^2$ configuration of Pr^{+3}, is a non-Kramers magnetic doublet. A similar scenario was proposed by Lyu et al. for a ferromagnetic semimetal PrAlSi [40].

Fig. 6(a) presents a map of the specific heat, showing its temperature and magnetic field dependence. There is a distinct boundary between the ferromagnetic state and the paramagnetic state. The additional white star-shaped points were calculated as the minima of $d\chi/dT$ curves for each of the applied magnetic fields. All those points closely follow the boundary established by the heat capacity measurements and validate both approaches. The influence of magnetic field is also presented in Fig. 6(b), where the anomaly is shown to decrease and shift toward slightly higher temperature as the applied magnetic field is increased.

The temperature dependence of the resistivity of Pr_7Ru_3, measured in zero applied field, is plotted in the main panel of Fig. 7. The metallic behavior of Pr_7Ru_3 is clearly visible, as the derivative $d\rho/dT$ is positive in the temperature range of 1.8–300 K. The slightly curvilinear behavior of resistivity above 50 K is likely due to a change in scattering as the population of one or more excited CEF levels changes. There is a sharp drop in resistivity near the transition temperature, corresponding to the ferromagnetic ordering of the Pr spins. Moreover, this drop tends to flatten with the increasing magnitude of the applied field, which is a sign of the magnetic origin of the transition. As shown in the inset, this drop is fully eliminated in the applied field of 5 T.

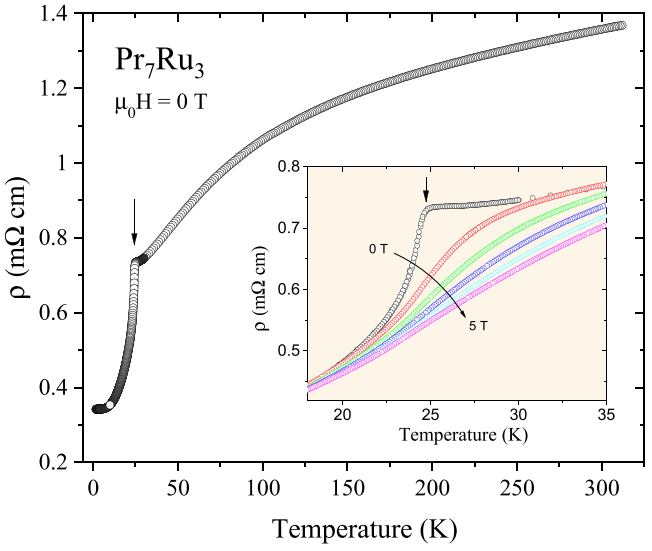

Fig. 7. Pr_7Ru_3 resistivity temperature dependence in zero applied field, with visible metallic behavior and ferromagnetic ordering transition near 25 K. The inset shows resistivity data in magnetic fields of 0–5 T.

4. Summary

Polycrystalline Pr_7Ru_3 was synthesized and its magnetic, transport, and thermal properties were measured. Structure data, obtained by the LeBail refinement of room temperature powder XRD data, gives values of the lattice constants: a = 7.3606(7) Å, b = 23.120(1) Å, and c = 6.5959(5) Å and is in agreement with the one reported in the literature [19]. Detailed analysis of the magnetic data for Pr_7Ru_3 indicates the occurrence of a ferromagnetic transition with the Curie temperature T_C = 24.5 K, determined from the heat capacity measurement. Above T_C the χ(T) data follow a modified Curie-Weiss law with a Curie-Weiss temperature Θ_{CW} = 30(1) K and effective magnetic moment 3.39(1) μ_B/Pr, which is close to the theoretical 3.58 μ_B/Pr value. Possible CEF level splittings at high temperature, as well as the finite 4 f spin-orbit coupling, might influence the fit and cause a small discrepancy.

Ferromagnetic behavior in Pr_7Ru_3 is seen via the hysteresis in the M(H) loop at low temperatures with the remnant magnetization μ_R = 0.6 μ_B mol-Pr^{-1} and the estimated coercivity field 0.08 T. Hence, Pr_7Ru_3 can be classified as a soft ferromagnet. Our heat capacity data confirm a bulk transition at about 24.5 K with a clear λ-like anomaly. The magnetic entropy S_{mag} released up to T_C is close to *R*ln2 and hence we suggest that the ground state for Pr_7Ru_3 is a non-Kramers magnetic doublet, as it was also reported for a ferromagnetic semimetal PrAlSi [40]. It is worth noting that the full magnetic entropy $S_{mag.}$ of the ninefold multiplets (*R*ln9) for Pr_7Ru_3 is released near room temperature.

Physical properties of the Pr-based intermetallic compounds in most cases reveal interesting, though complex behavior and Pr_7Ru_3 is not an exception. A neutron diffraction study would prove valuable to elucidate the magnetic structure of Pr_7Ru_3. The existence of four inequivalent Pr positions in the unit cell, each having different coordination (different local site symmetry) will cause a complicated crystal field splitting of Pr^{+3}. In order to shed light on the overall splitting energies, inelastic neutron scattering measurements are required.

Pr_7Ru_3 is the first ferromagnetic compound in the RE_7Ru_3 family and what is also important does not contain 3*d* metal. Observed ferromagnetism, with a relatively high T_C = 24.5 K, develops in a CEF ground state doublet. If one makes hypothetical RE_7Os_3 compounds, which are likely to be magnetic, then the interplay of spin-orbit coupling and magnetism can be studied in detail in this complex, yet interesting system.

CRediT authorship contribution statement

S. Królak: Conceptualization, Writing – original draft. **H. Świątek:** Conceptualization, Writing – original draft. **K. Górnicka:** Visualization. **M.J. Winiarski:** Data curation, Formal analysis. **W. Xie:** Formal analysis, Writing – review & editing, Resources. **R.J. Cava:** Formal analysis, Resources, Writing – review & editing. **T. Klimczuk:** Formal analysis, Visualization, Resources, Writing – review & editing, Supervision.

Data Availability

Data will be made available on request.

Declaration of Competing Interest

The authors declare the following financial interests/personal relationships which may be considered as potential competing interests: Tomasz Klimczuk reports financial support was provided by National Science Centre Poland. Robert J. Cava reports financial support was provided by Division of Basic Energy Sciences of the US Department of Energy. Weiwei Xie reports financial support was provided by Division of Basic Energy Sciences of the US Department of Energy.

Acknowledgements

The work at GUT was supported by the National Science Centre (Poland; Grant UMO-2018/30/M/ST5/00773), at Princeton University by the Division of Basic Energy Sciences of the US Department of Energy grant DE-FG02–98ER45706. The work at Rutgers was supported by DOE under the contract of DE-SC0022156. TK acknowledges Joe D. Thompson (LANL) for valuable discussion and comments to the manuscript.

Appendix A. Supporting information

Supplementary data associated with this article can be found in the online version at doi:10.1016/j.jallcom.2022.167279.

References

[1] R. Nakabayashi, Y. Tazuke, S. Murayama, Itinerant electron weak ferromagnetism in Y2Ni7 and YNi3, J. Phys. Soc. Jpn. 61 (1992) 774.
[2] D. Gignoux, R. Lemaire, P. Molho, F. Tasset, Magnetism resurgence in the Y-Ni alloys studied on the YNi3 compound, J. Magn. Magn. Mater. 15–18 (1980) 289.
[3] A.D. Chinchure, E. Muñoz Sandoval, J.A. Mydosh, Metamagnetism and giant magnetoresistance of the rare-earth intermetallic compounds R 2 Ni 2 Pb (R = Er, Ho, Dy), Phys. Rev. B 66 (2002) 020409.
[4] R. Rajivgandhi, J. Arout Chelvane, S. Quezado, S.K. Malik, R. Nirmala, Effect of rapid quenching on the magnetism and magnetocaloric effect of equiatomic rare earth intermetallic compounds RNi (R = Gd, Tb and Ho), J. Magn. Magn. Mater. 433 (2017) 169.
[5] B. Das, R. Choudhary, R. Skomski, B. Balasubramanian, A.K. Pathak, D. Paudyal, D.J. Sellmyer, Anisotropy and orbital moment in Sm-Co permanent magnets, Phys. Rev. B 100 (2019) 024419.
[6] H. v Löhneysen, H. Bartolf, S. Drotziger, C. Pfleiderer, O. Stockert, D. Souptel, W. Löser, G. Behr, Rare-earth intermetallic compounds at a magnetic instability, J. Alloy. Compd. 408–412 (2006) 9.
[7] T. Tsutaoka, Y. Nakamori, Ferromagnetic properties of Ce7Rh3 and Pr7Rh3 single crystals, J. Alloy. Compd. 452 (2008) 210.
[8] J. Strychalska, M. Roman, Z. Sobczak, B. Wiendlocha, M.J. Winiarski, F. Ronning, T. Klimczuk, Physical properties and electronic structure of La 3 Co and La 3 Ni intermetallic superconductors, Phys. C: Supercond. Its Appl. 528 (2016) 73.
[9] S.B. Roy, P. Chaddah, Anomalous superconducting properties in CeRu 2: effects of magnetic and nonmagnetic substitutions, Phys. Rev. B 55 (1997) 11100.
[10] F.Y. Fradin, H.B. Radousky, N.J. Zaluzec, G.S. Knapp, J.W. Downey, Superconductivity in the Y▢Ir system, Mater. Res. Bull. 17 (1982) 427.

[11] K. Górnicka, R.J. Cava, T. Klimczuk, The electronic characterization of the cubic laves-phase superconductor CaRh2, J. Alloy. Compd. 793 (2019) 393.
[12] D. Singh, M.S. Scheurer, A.D. Hillier, D.T. Adroja, R.P. Singh, Time-reversal-symmetry breaking and unconventional pairing in the noncentrosymmetric superconductor La 7 Rh 3, Phys. Rev. B 102 (2020).
[13] S. Niitaka, E. Minamitani, Y. Kim, H. Takagi, K. Kono, Comprehensive macroscopic investigation on hexagonal C14 Laves-Type Ru-Based superconductors A Ru_2 (A = Lu, Y, Sc) with effective electron correlation, J. Phys. Soc. Jpn. 82 (2013) 124703.
[14] A. Bhattacharyya, D.T. Adroja, P.K. Biswas, Y.J. Sato, M.R. Lees, D. Aoki, A.D. Hillier, *Ir* 5 d -Band derived superconductivity in $LaIr_3$, J. Phys.: Condens. Matter 32 (2020) 065602.
[15] S. Gutowska, K. Górnicka, P. Wójcik, T. Klimczuk, B. Wiendlocha, Strong-coupling superconductivity of SrIr 2 and SrRh 2: phonon engineering of metallic Ir and Rh, Phys. Rev. B 104 (2021).
[16] G. Srinivas, V. Sankaranarayanan, S. Ramaprabhu, Kinetics of hydrogen absorption in Ho1−xMmxCo2 alloys, J. Alloy. Compd. 448 (2008) 159.
[17] Y. Zhang, et al., Transitions from a Kondo-like diamagnetic insulator into a modulated ferromagnetic metal in $FeGa_{3-y}$ Ge_y, Proc. Natl. Acad. Sci. U. S. A 115 (2018) 3273.
[18] Y. Hadano, S. Narazu, M.A. Avila, T. Onimaru, T. Takabatake, Thermoelectric and magnetic properties of a narrow-gap semiconductor FeGa 3, J. Phys. Soc. Jpn. 78 (2009) 013702.
[19] A. Palenzona, F. Canepa, New compounds in the 30–40 at % Ru range of the rare earth-ruthenium (R-Ru) systems, J. Less Common Met. 162 (1990) 267.
[20] P. Pedrazzini, G. Schmerber, M. Gómez Berisso, J.P. Kappler, J.G. Sereni, Magnetic and superconducting properties of A7B3 compounds (A=Th or La and B=Ni, Co, Fe or Pd, Rh, Ru), Phys. C: Supercond. 336 (2000) 10.
[21] J.G. Sereni, O. Trovarelli, G. Schmerber, J.P. Kappler, Non-fermi-liquid signatures in stoichiometric Ce7Ru3 at ambient pressure, Phys. B: Condens. Matter 259–261 (1999) 405.
[22] S. Ahamed, R. Moessner, O. Erten, Why rare-earth ferromagnets are so rare: insights from the p -Wave kondo model, Phys. Rev. B 98 (2018).
[23] M.L. Fornasini, A. Palenzona, Sr7Pt3: an orthorhombic structure formed by Pt-centered trigonal prisms, J. Solid State Chem. 47 (1983) 30.
[24] J. Jensen , A. Mackintosh , 1991. Rare Earth Magnetism: Structures and Excitations. (Clarendon Press, 1991).
[25] N. Takeda, M. Ishikawa, The Ferromagnetic Kondo-Lattice compound $SmFe_4P_{12}$, J. Phys.: Condens. Matter 15 (2003) L229.
[26] L. Li, et al., Coexistence of Superconductivity and Ferromagnetism in Sr 0.5 Ce 0.5 FBiS 2, Phys. Rev. B 91 (2015) 014508.
[27] V.A. Kulbachinskii, A.Yu Kaminskii, K. Kindo, Y. Narumi, K. Suga, P. Lostak, P. Svanda, Ferromagnetism in new diluted magnetic semiconductor Bi2−Fe Te3, Phys. B: Condens. Matter 311 (2002) 292.
[28] C. Krellner, N.S. Kini, E.M. Brüning, K. Koch, H. Rosner, M. Nicklas, M. Baenitz, C. Geibel, CeRuPO: a rare example of a ferromagnetic kondo lattice, Phys. Rev. B 76 (2007).
[29] N.S. Kini, A.M. Strydom, H.S. Jeevan, C. Geibel, S. Ramakrishnan, Transport and Thermal Properties of Weakly Ferromagnetic Sr_2IrO_4, J. Phys.: Condens. Matter 18 (2006) 8205.
[30] D. Schray, G. Abbas, Y. Lan, V. Mereacre, A. Sundt, J. Dreiser, O. Waldmann, G.E. Kostakis, C.E. Anson, A.K. Powell, Combined magnetic susceptibility measurements and ^{57}Fe mössbauer spectroscopy on a ferromagnetic $\{Fe^{III}_4Dy_4\}$ Ring, Angew. Chem. Int. Ed. 49 (2010) 5185.
[31] C.-K. Tian, C. Wang, W. Ji, J.-C. Wang, T.-L. Xia, L. Wang, J.-J. Liu, H.-X. Zhang, P. Cheng, Domain wall pinning and hard magnetic phase in Co-Doped bulk single crystalline Fe 3 GeTe 2, Phys. Rev. B 99 (2019).
[32] L. Li, O. Niehaus, M. Kersting, R. Pöttgen, Magnetic properties and magnetocaloric effect in the rare earth-rich phases RE4PtMg (RE = Ho and Er), Intermetallics 62 (2015) 17.
[33] K.H. Mader, E. Segal, W.E. Wallace, Magnetic and crystallographic characteristics of (Pr,La)Al3, (Pr,Y)Al3, (Pr,La)Al2 and (Pr,Y)Al2, J. Phys. Chem. Solids 30 (1969) 1.
[34] V. Goruganti, K.D.D. Rathnayaka, J.H. Ross, Y. Öner, C.S. Lue, Y.K. Kuo, Transport and magnetic properties of NdCuGe compound, J. Appl. Phys. 103 (2008) 073919.
[35] K. Marumoto, F. Takayama, Y. Miyako, Crystal-field splitting of praseodymium in the dilute system (PrxLa 1− x)Ru2Si2, J. Magn. Magn. Mater. 177–181 (1998) 353.
[36] B. Barbara, D. Gignoux, C. Vettier, Lectures on Modern Magnetism (1988, n.d.).
[37] A.K. Pathak, D. Paudyal, Y. Mudryk, K.A. Gschneidner, V.K. Pecharsky, Anomalous schottky specific heat and structural distortion in ferromagnetic PrAl 2, Phys. Rev. Lett. 110 (2013) 186405.
[38] A. Rudenko, Z. Henkie, T. Cichorek, Low-temperature specific heat and magnetic properties of the filled skutterudite ferromagnet NdRu4As12, Solid State Commun. 242 (2016) 21.
[39] T. Cichorek, A. Rudenko, P. Wiśniewski, R. Wawryk, L. Kępiński, A. Pietraszko, Z. Henkie, Schottky-like anomaly on the border of localized ferromagnetism in the filled skutterudite NdOs 4 As 12, Phys. Rev. B 90 (2014) 195123.
[40] M. Lyu, J. Xiang, Z. Mi, H. Zhao, Z. Wang, E. Liu, G. Chen, Z. Ren, G. Li, P. Sun, Nonsaturating magnetoresistance, anomalous hall effect, and magnetic quantum oscillations in the ferromagnetic semimetal PrAlSi, Phys. Rev. B 102 (2020).